

# Enhanced FCME Thresholding for Wavelet-Based Cognitive UWB over Fading Channels

Haleh Hosseini, Norsheila Fisal, and Sharifah Kamilah Syed-Yusof

*The cognitive ultra-wideband (UWB) network detects interfering narrowband systems and adapts its configuration accordingly. An inherently adaptive and flexible candidate for cognitive UWB transmission is the wavelet packet multicarrier modulation (WPMCM). In this letter, we use an enhanced forward consecutive mean excision thresholding algorithm to tackle the noise uncertainty in the wavelet-based sensing of WPMCM systems, and mathematical analysis is performed for primary user channel fading. As a benchmark, we compare the proposed system with a conventional fast Fourier transformation-based system, and performance investigation proves significant improvements when primary and secondary links are subjected to multipath fading and noise.*

*Keywords: Channel fading, cognitive ultra-wideband, forward consecutive mean excision, spectrum sensing, wavelet packet transform.*

## I. Introduction

Development of high data rate wireless links and efficient spectrum utilization has motivated the combination of ultra-wideband (UWB) and cognitive radio as a promising technique. UWB spectrum, respecting regulations of Federal Communications Commission, is allocated from 3.1 GHz to 10.6 GHz for underlying usage. This bandwidth is divided into five groups of 528 MHz subbands for multiband UWB. Each subband consists of 128 subcarriers with 4.125 MHz tone spacing. The very low transmission power, large bandwidth, and unlicensed nature of UWB systems lead to coexistence with primary or licensed narrowband systems, which may jam

the receiver completely. Narrowband interference (NBI) bandwidth occupies less than 50% of total signal bandwidth. Detection of these potential NBI links requires a library of system features that vary in different countries and need to be updated to include new systems [1]. To avoid mutual interference with these licensed users, cognitive UWB performs spectrum sensing, that is, it detects primary users by energy detector (ED) and vacates the occupied channels at a certain period of time. Proper thresholding is a major challenge of ED. In [2], wavelet packet-based multicarrier modulation (WPMCM) has been used instead of OFDM for cognitive UWB systems to suppress side-lobes effect and lower inter-symbol interference and inter-channel interference. Among various sensing schemes, wavelet packet-based methods are inherently suitable for WPMCM due to their embedded wavelet packet transform (WPT) engine and minimal requirement of system modification. However, severe channel fading, hidden nodes, and shadowing can affect accurate decision making of sensing phase.

In this letter, WPT-based ED is proposed for cognitive multiband (MB)-WPMCM UWB systems. We present mathematical analysis of the detection problem with the primary user channel effects. The forward consecutive mean excision (FCME) combined with localization based on double thresholding (LAD) algorithms, so-called enhanced FCME, is applied, and a deactivation vector is produced to feed a secondary transmitter and allocate the corresponding spectrum for data transmission. Simulation results represent reduced errors and higher decision accuracies over various primary and secondary user channel fading and noise conditions. Particularly low BERs are achieved with multipath UWB channel models (CMs) for IEEE 802.15.3a on the proposed system compared to the conventional system.

Manuscript received Feb. 6, 2011; revised Apr. 5, 2011; accepted Apr. 25, 2011.

Haleh Hosseini (phone: +60 177283683, email: halehsi@fkegraduate.utm.my), Norsheila Fisal (email: sheila@fke.utm.my), and Sharifah Kamilah Syed-Yusof (email: kamilah@fke.utm.my) are with the Department of Electrical Engineering, Universiti Teknologi Malaysia, Johor, Malaysia.

<http://dx.doi.org/10.4218/etrij.11.0211.0046>

## II. System Description

The ability to sense the environment enables cognitive UWB to exploit spectral opportunities, perform spectrum shaping, and adapt its data rate, bandwidth, and transmit power, accordingly. The cognitive radio system and its corresponding channels in frequency domain are shown in Fig. 1. The received signal vector at the primary and secondary RX is

$$\begin{bmatrix} Y_p \\ Y_c \end{bmatrix} = \begin{bmatrix} H_{11} & H_{12} \\ H_{21} & H_{22} \end{bmatrix} \begin{bmatrix} S_p \\ S_c \end{bmatrix} + \begin{bmatrix} V_p \\ V_c \end{bmatrix}, \quad (1)$$

where  $S_p$  is primary user's transmitted signal and  $S_c$  is the cognitive user's transmitted signal. The complex Gaussian noises at the primary and cognitive receivers are  $V_p \sim c\mathcal{N}(0, \sigma_{V_p}^2)$  and  $V_c \sim c\mathcal{N}(0, \sigma_{V_c}^2)$ , respectively. Channel gains are defined as  $H_{ij}$ , while  $Y_p$  and  $Y_c$  denote signals at primary and cognitive receivers, respectively.

During the sensing interval, the cognitive transmitter is off and sensing problem for the receiver can be formulated as a binary hypothesis testing problem, in which  $\mathcal{H}_0$  shows the absence of primary user and  $\mathcal{H}_1$  shows the presence case. Denote  $\gamma = |H_{21}|^2 \sigma_{S_p}^2 / \sigma_{V_c}^2$  as the received signal-to-noise ratio (SNR) of primary user under the hypothesis of  $\mathcal{H}_1$  ( $\sigma^2$  is variance). We consider the test statistic as

$$T(y_c) = 1/N \cdot \sum_{n=1}^N |y_c[n]|^2. \quad (2)$$

The procedure for energy detection requires a priori knowledge of the noise power to provide the comparison of

$$T(y_c) \underset{\mathcal{H}_1}{>} \underset{\mathcal{H}_0}{<} \lambda, \quad (3)$$

for the test threshold  $\lambda$ . Probability distribution function of  $T(y_c)$  can be approximated as Gaussian random process function due to central limit theorem for asymptotically large  $N$  ( $>250$ ). Then,  $T(y_c) \sim \mathcal{N}(\mu_i, \sigma_i^2)$ ,  $i=0, 1$ , and its mean and variance are given as

$$\mathcal{H}_0 : \begin{cases} \mu_0 = \sigma_{V_c}^2, \\ \sigma_0^2 = \frac{1}{N} \sigma_{V_c}^4, \end{cases} \quad \mathcal{H}_1 : \begin{cases} \mu_1 = (\gamma + 1) \sigma_{V_c}^2, \\ \sigma_1^2 = \frac{1}{N} (\gamma + 1)^2 \sigma_{V_c}^4, \end{cases} \quad (4)$$

when both the noise and signal are circularly symmetric complex Gaussian variables [3]. The corresponding probabilities of false alarm and detection in the threshold test are given as

$$P_{fa} = \Pr(T(y_c) > \lambda | \mathcal{H}_0) = Q\left(\frac{\lambda - \sigma_{V_c}^2}{\sigma_{V_c}^2 / \sqrt{N}}\right), \quad (5)$$

$$P_d = \Pr(T(y_c) > \lambda | \mathcal{H}_1) = Q\left(\frac{\lambda - (\gamma + 1) \sigma_{V_c}^2}{(\gamma + 1) \sigma_{V_c}^2 / \sqrt{N}}\right), \quad (6)$$

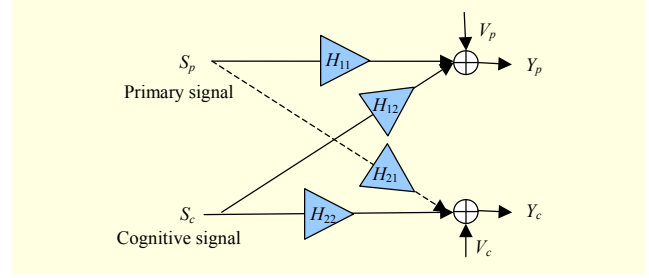


Fig. 1. Interfering primary channel represented by dashed lines.

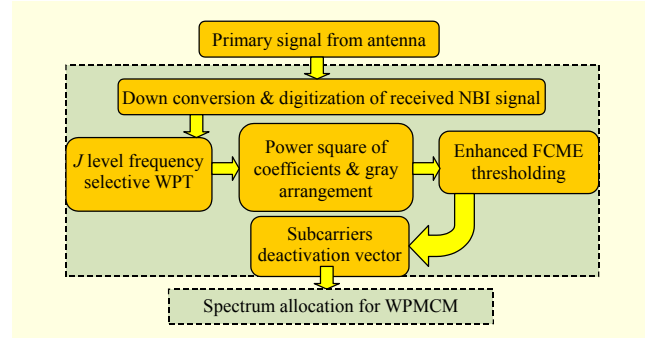


Fig. 2. Proposed sensing system.

where Q-function is the tail probability of standard normal distribution. Wavelet-based ED is flexible, able to deal with both narrowband and wideband sources in variable channel conditions, and more attractive than periodogram and Welch approaches [4]. WPT recursively decomposes the spectrum into different subbands and provides time-frequency resolution trade-offs.

The block diagram of our proposed wavelet-based sensing system is depicted in Fig. 2. First, a received signal is down-converted and digitized, then transformed by WPT with a  $J$  level filter bank, where the number of output subcarriers is expressed as  $F=2^J$ . Due to Parseval's theorem, we obtain

$$T(y_c) = \frac{1}{N} [\sum_j \sum_k a_{j,k}^2 + \sum_j \sum_k d_{j,k}^2], \quad (7)$$

where  $a_{j,k}$  is the scaling coefficient,  $d_{j,k}$  is the wavelet coefficient, and  $j$  shows the level of transform. The number of succession  $J$  is limited by frequency resolution and computational power. The output of every wavelet packet node at every level can be chosen according to the desired frequency resolution. The power square of the coefficients represents interference energy at a specified frequency or subcarrier. Note that the frequencies of these coefficients are ordered by a sequential binary gray code value and need rearrangement. This decision rule, shown in (3), will be used in our proposed WPT-based spectrum sensing for cognitive WPMCM UWB. The transmitted signal waveform is adaptively shaped by deactivating occupied subcarriers and utilizing the spectrum holes.

### III. Enhanced FCME Thresholding Algorithm

The limitation of the energy detector is its dependency on prior knowledge of the noise power, which is usually unknown in a varying environment. Constant false alarm rate (CFAR) techniques are used to tackle with this problem. FCME algorithm is an adaptive and iterative forward CFAR method to estimate the noise level and set the threshold. For a zero mean complex Gaussian random noise, the magnitude square of  $i$ -th WPT subcarrier of the received signal  $\|Y_i\|^2$  follows central chi-squared distribution, and FCME parameter  $T_{\text{CME}}$  is the solution to

$$P_{fa} = e^{-T_{\text{CME}} \cdot M} \sum_{k=0}^{M-1} \frac{1}{k!} (T_{\text{CME}} \cdot M)^k, \quad (8)$$

where  $M$  is the dimension of  $Y_i$  vector [5]. Then, FCME algorithm can be performed as following next steps:

i) For a large number of subcarriers,  $I \rightarrow \infty$ , compute parameter  $T_{\text{CME}}$  as

$$T_{\text{CME}} = \begin{cases} -\ln(P_{fa}), M = 1, \\ \text{FINV}(1 - P_{fa}, 2M, 2M(I-1)), M > 1, \end{cases} \quad (9)$$

where  $P_{fa}$  is a desired false alarm probability and  $\text{FINV}$  is the inverse of the Fisher cumulative distribution function.

ii) Rearrange samples of  $Y_i$  according to  $\|Y_i\|^2$  in the ascending order, denoted as  $\{Z_i\}_{i=1}^I$ . Assuming  $Q_i = \|Z_i\|^2$ , form the initial clean set with size  $K$ , typically 10% of total set size.

iii) Compute  $T_k = \frac{1}{K} \cdot \sum_{i=1}^K Q_i \cdot T_{\text{CME}}$ .

iv) Find all members of the set  $\{Z_i\}_{i=K+1}^I$  in which  $Q_i$  is smaller than  $T_k$ , increase the initial clean set size  $K$  accordingly, and go to iii). If new members do not exist, samples below the threshold are set as noise and the algorithm is finished.

For the LAD algorithm, FCME is run twice with two threshold parameters. In contrast with other blind sensing methods, the enhanced FCME algorithm, which is combined with LAD processing, is able to localize the bandwidth and center frequency of interference. LAD blindly detects number and location of concentrated interfering signals as clusters.

To accomplish the enhanced FCME algorithm, the lower and upper thresholds are calculated for two desired values of  $P_{lfa}$  and  $P_{u fa}$ . Then, FCME algorithm is performed for lower threshold, and adjacent samples above the lower threshold are grouped into the same clusters. When at least the sample with maximum energy is above the upper threshold, the cluster is accepted as primary system interference. In practice,  $P_{fa}$  and  $P_d$  are metrics for evaluation of the algorithm performance as

$$\mathcal{H}_0 : P_{fa} = \left( \sum_c \hat{l}_{0,c} / I - L \right), \quad \mathcal{H}_1 : P_d = \left( \sum_c \hat{l}_{1,c} / L \right), \quad (10)$$

where  $L$  is the total number of occupied subcarriers,  $\hat{l}_{0,c}$  and  $\hat{l}_{1,c}$  represent the number of falsely detected and correctly detected subcarriers in  $c$ -th cluster, respectively. Normalized mean square error for the estimated bandwidth  $\hat{B}$  of detected signal is defined as

$$E \left| \hat{B} - B \right|^2 / B^2. \quad (11)$$

### IV. Numerical Results and Discussion

We evaluated the developed system by MATLAB simulation and compared with fast Fourier transformation (FFT)-based ED for OFDM as a conventional method; FCME is considered in both systems. We generate primary signal with varying bandwidths at the center frequency of  $f_c = 264$  MHz, using a linear band-pass FIR filter driven by unit variance white Gaussian noise at the input. According to the MB-UWB, we consider the number of subcarriers  $I$  equal to 128, and NBI as random data fed to sensing block through an AWGN channel. A frequency selective filter is applied for WPT engine at the sensing part and transceiver side. The wavelet filters are implemented by the modified Remez exchange algorithm [6]. Their parameters are set as the length of filter,  $L=50$ , regularity order,  $K=19$ , and transition bandwidth,  $B=0.1$ . We assume that the channel state information provided by sensing part is available at both cognitive transmitter and receivers.

Figure 3 compares power spectrum density of detected signals achieved by FFT-based (128 bins) and WPT (7 level)-based energy detectors. Interference to noise ratio (INR) is equal to 0 dB, and the graphs represent higher side-lobes suppression and less variance for WPT sensing compared to FFT-based for NBI with both 4% and 24% occupied bandwidths. This detected interfering signal is analyzed by enhanced FCME algorithm to identify thresholds and determine deactivation subcarrier vector.

Figure 4 investigates the probability of false alarm and the probability of detection for the proposed and conventional sensing procedures. The number of tested subcarriers is 128, and NBI bandwidth varies from 4% to 24% of total bandwidth. These graphs show that the new method successfully controls the false alarm rate around 0.02 and significantly enhances the detection rate near 1 for varying INR from -10 dB to +10 dB. The outcome of this phase is the deactivation vector for WPMCM transceiver with 128 subcarriers due to MB-UWB standard. According to Fig. 5, when a primary user channel is Rician or Rayleigh, about 10-dB SINR improvement is obtained by the proposed system at BER of  $10^{-2}$ . Figure 6

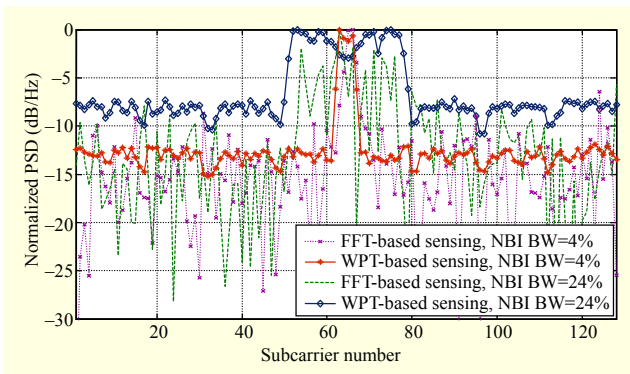


Fig. 3. Power spectral density of primary users with 4% and 24% bandwidth of 128 cognitive subcarriers (INR=0 dB).

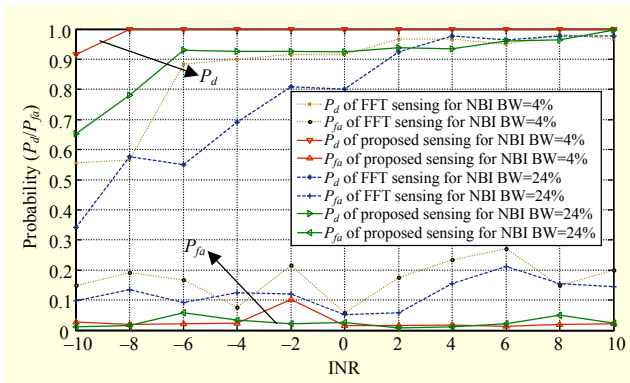


Fig. 4. Comparison between probability of detection and false alarm.

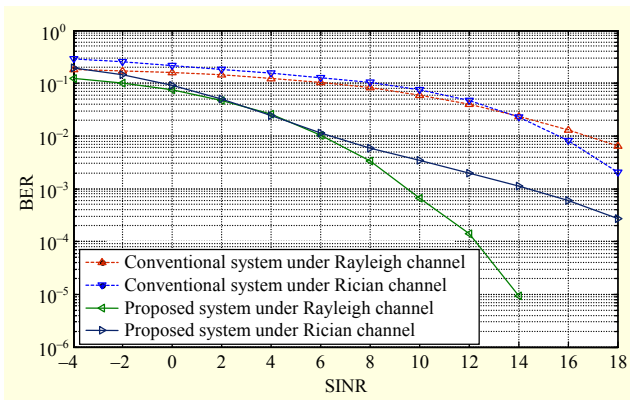


Fig. 5. BER comparison at different primary channel conditions (INR= 10 dB, NBI BW=4%).

surveys the effect of cognitive UWB CMs on the conventional and the proposed systems. We consider perfect channel estimation, and a simulation is performed using impulse response models of the indoor multipath (IEEE 802.15.3a) based on Saleh-Valenzuela model with lognormal fading. The results show significant enhancement under different UWB channel conditions. For instance, at BER of  $10^{-5}$ , SNR

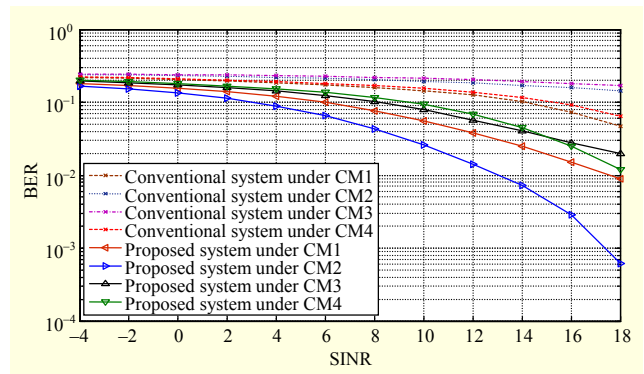


Fig. 6. BER comparison at different UWB channel conditions (INR= 10 dB, NBI BW=4%).

reaches to 8 dB less than the conventional system for CM1.

## V. Conclusion

In this letter, an analytical sensing problem, considering primary user channel effects, has been presented, and enhanced FCME thresholding algorithm is applied for wavelet packet-based spectrum sensing under noise uncertainty. This approach is specifically recommended for cognitive MB-WPMCM UWB due to the existence of wavelet engines towards coming flexible communication technology. The numerical results, with various metrics of performance analysis, verify that this method outperforms the traditional system over the primary and secondary link fading. In future work, we intend to survey CFAR methods and experimental measurement.

## References

- [1] A.M. Rateb, S.K. Syed-Yusof, and N. Faisal, "Improvement of Ultra-wideband Link Performance over Bands Requiring Interference Mitigation in Korea," *ETRI J.*, vol. 32, no. 1, Feb. 2010, pp. 44-52.
- [2] H. Hosseini, N.B. Faisal, and S.K. Syed-Yusof, "Wavelet Packet Based Multicarrier Modulation for Cognitive UWB Systems," *SPIJ.*, vol. 4, no. 2, May 2010, pp. 75-84.
- [3] Y.C. Liang et al., "Sensing-Throughput Tradeoff for Cognitive Radio Networks," *ICC*, Glasgow, 2007, pp. 5330-5335.
- [4] D.D. Ariananda, M.K. Lakshmanan, and H. Nikookar, "A Study on the Application of Wavelet Packet Transforms to Cognitive Radio Spectrum Estimation," *CrownCom*, June 2009, pp. 1-6.
- [5] J. Lehtomaki et al., "CFAR Outlier Detection with Forward Methods," *IEEE Trans. Signal Process.*, vol. 55, no. 9, Sept. 2007, pp. 4702-4706.
- [6] O. Rioul and P. Duhamel, "A Remez Exchange Algorithm for Orthonormal Wavelets," *IEEE Trans. Circuits Syst. II*, vol. 41, no. 8, Aug. 1994, pp. 550-560.